García-Ballesteros, S.; Constante, M.; Vicente Candela, R.; Mora Carbonell, M.; Amat Payá, AM.; Arqués Sanz, A.; Carlos, L.... (2017). Humic-like substances from urban waste as auxiliaries for photo-Fenton treatment: a fluorescence EEM-PARAFAC study. Photochemical & Photobiological Sciences. 16:38-45. doi:10.1039/c6pp00236f

Humic-like Substances from Urban Waste as Auxiliaries for Photo-Fenton Treatment: a Fluorescence EEM-PARAFAC Study

S. García Ballesteros[a], M. Costante[b], R. Vicente[a], M. Mora[c], A. M. Amat[a], A. Arques[a], L. Carlos[d]* and F.S. García Einschlag[b]

[a] Grupo de Procesos de Oxidación Avanzada, Dpto de Ingeniería Textil y Papelera, Universidad Politécnica de Valencia. Plaza Ferrándiz y Carbonell s/n, Alcoy, Spain.

[b] Instituto de Investigaciones Fisicoquímicas Teóricas y Aplicadas (INIFTA), CCT-La Plata-CONICET, Universidad Nacional de La Plata, Diag 113 y 64, La Plata, Argentina.

[c] Grupo de Procesos de Oxidación Avanzada, Dpto de Matemática Aplicada, Universidad Politécnica de Valencia. Plaza Ferrándiz y Carbonell s/n, Alcoy, Spain.

[d] Instituto de Investigación y Desarrollo en Ingeniería de Procesos, Biotecnología y Energías alternativas, PROBIEN (CONICET-UNCo), Buenos Aires 1400, Neuquén, Argentina.

* To whom correspondence should be addressed. (L. Carlos) Phone: +54 299 4490300. E-mail: luciano.carlos@probien.gob.ar. Postal address: Buenos Aires 1400 (CP 8300), Neuquén, Argentina.

Abstract

In this work, analysis of excitation−emission-matrices (EEM) has been employed to gain further insight into the characterization of humic like substances (HLS) obtained from urban wastes (soluble bio-organic substances, SBOs). In particular, complexation of these substances with iron and changes along a photo-Fenton process have been studied. Recorded EEMs were decomposed by using parallel factor analysis (PARAFAC). Three fluorescent components were identified by PARAFAC modeling of the entire set of SBO solutions studied. The EEM peak locations ($\lambda_{ex}/\lambda_{em}$) of these components were (310-330) nm / (400-420) nm (C1), (340-360) nm / (450-500) nm (C2), 285 nm / (335-380) nm (C3). Slight variations of the maximum position of each component with the solution pH were observed. The interaction of SBO with Fe(III) was characterized by determining the stability constants of the components with Fe(III) at different pH values, which were in the order of magnitude of the ones reported for humic substances and reached their highest values at pH = 5. Photochemical experiments employing SBO and Fe(III), with and without H_2O_2, showed pH-dependent trends for the evolution of the modeled components, which exhibited a strong correlation with the efficiency reported for the photo-Fenton processes in the presence of SBO at different pH values.

Introduction

Photo-Fenton is an advanced oxidation process (AOP) that is receiving increasing attention from researchers. Its oxidative action is a result of the formation of reactive oxygen species, especially hydroxyl radicals ($HO^{\bullet}$), that are able to oxidize

most of organic pollutants.[1-2] Despite its advantages of being economic and environmental friendly, photo-Fenton reaction has not been widely used because of the requirement of acidic conditions (optimal pH 2.8), since at higher pH values the formation of non-active iron oxides or hydroxides substantially decreases the efficiency of pollutant removal.[3] Interest has grown over the past few years, in the application of circumneutral photo-Fenton processes for wastewater treatment.[4-5] An approach to avoid acidification and ferric iron hydroxide precipitation is performing the reaction with complexing agents. It has been demonstrated that Fe(III) can be strongly complexed with different polydentate ligands.[6] Humic substances (HS) are among the materials employed for this purpose, because of their ability for iron complexation.[7-8] On the other hand, experimental results seem to prove that HS under UV-Vis irradiation can directly improve the degradation of pollutants by speeding up the redox cycling of iron due to ligand to metal charge transfer (LMCT) reactions of their ferric complexes, thus accelerating the photo-Fenton mechanism.[9-10] Nevertheless, the role played by HS in the oxidation mechanism is still not fully understood.

Recently, humic like substances (HLS), and in particular those isolated from the organic fraction of solid urban wastes (SBO, acronym of soluble bio-organic substances), have been successfully applied as iron complexing agent in photo-Fenton at slightly acidic pH.[11-12] Indeed, solar-photo-Fenton process in the presence of SBO have shown to be able to remove a mixture of emerging pollutants at pH 5.2, with an acceptable loss of efficiency when compared with pH 2.8 in the absence of SBO.[13] The capacity of HLS to expand the pH range up to ca. 5 in photo-Fenton processes might be ruled by the interaction of this substances with Fe(III). Also the transformation of HLS under UV-Vis irradiation could play a significant role on the efficiency of the Photo-Fenton process, as changes in the structure of those substances have been observed.[14] In fact, preliminary experiments carried out with SBO along a photo-Fenton process show that significant changes in their structure occurred, what resulted in some variation in their ability to drive mild photo-Fenton.[15] However, gaining further insight into mechanistic aspects of systems where HLS are involved is not easy, because their intrinsic complexity does not allow application of routine analytical methods. In this context, fluorescence excitation emission matrix (EEM) spectroscopy seems a promising alternative when dealing with such organic complex molecules. EEM spectroscopy is a simple, sensitive, and nondestructive analytical technique, commonly employed in the analysis of dissolved organic matter (DOM), that provides meaningful information on the molecular structure, functional groups, as well as intramolecular and intermolecular interactions with metallic ions.[16] Multivariate data analysis techniques are increasingly used to obtain quantitative information from EEMs. The most widely

used technique, parallel factor analysis (PARAFAC), deconvolutes complex EEMs into independent fluorescent components which represent groups of similar fluorophores for both quantitative and qualitative analysis.[17] Fluorescence EEM-PARAFAC technique has been used to characterize DOM in natural aqueous ecosystems as well as in wastewaters.[18-19] In particular, Yang et al.[20] investigated sunlight-induced changes in fluorophores of wastewater-derived organic matter with different salinities using EEM-PARAFAC; this application might be of interest in order to monitor changes in HLS when submitted to a photo-degradation process, as shown in a previous work.[14] On the other hand, combining fluorescence quenching titrations with EEM-PARAFAC is a potentially useful technique in the assessment of interaction constants between dissolved metals and DOM.[21-22]

With this background, the aim of this work was to investigate whether fluorescence EEM-PARAFAC technique can be a useful tool to gain further insight into the complexation of iron with organic macromolecules, which is a necessary step in order to understand mechanistic issues of mild photo-Fenton driven in the presence of these substances. In particular, both the interaction of SBO with Fe(III) and the transformation of these substances during the photo-Fenton processes at different pHs using fluorescence have been investigated.

Experimental

Reagents.

$FeCl_3x6H_2O$ and H_2O_2 (30% w/v) were purchased from Panreac. All aqueous solutions were prepared with ultra-pure water, obtained from a Millipore Milli-Q™ system. SBO were kindly provided by Alessandra Bianco Prevot and Enzo Montoneri, from University of Torino. They were isolated from urban biowastes sampled from the process lines of ACEA Pinerolese waste treatment plant in Pinerolo (Italy). The urban biowaste was obtained in the compost production section, from urban public park trimming and home gardening residues aged for more than 180 days. Isolation of SBO was performed following a previously reported procedure.[12] SBO chemical structure is fully detailed elsewhere.[23]

Experimental conditions.

Solution of 20 mg/L of SBO combined with solutions of Fe(III) at different concentrations (1 - 10 mg/L) were used for fluorescence quenching titrations experiments, which were carried out at three different pH (3, 5 and 7). To study the evolution of SBO in photo-Fenton processes, a solution of 20 mg/L of SBO and 5 mg/L of Fe(III), with (2,2 mmol/L) and without H_2O_2 were used. These concentrations were selected as they are close to the optimal condition previously reported for the degradation of a mixture of emerging pollutant in the presence of SBO at pH

5.[12] Photo-Fenton experiments were carried out in a 250 mL cylindrical Pyrex vessel irradiated with a solar simulator (Sun 2000, ABET Technologies) equipped with a 550 W Xenon Short Art Lamp. A pyrex glass filter was used to cut off radiation below 300 nm.

Analytical Techniques.

The fluorescence Excitation Emission Matrices (EEMs) were recorded with a modular QuantaMaster spectrofluorometer and collected by subsequent scanning emission from 300 to 600 nm at 5 nm increments by varying the excitation wavelength from 250 to 550 nm at 5 nm increments. Data at lower excitation wavelengths were not recorded because of the excessive background noise, caused by the low intensity of the lamp in the range of 200 - 250 nm. The spectra were recorded using excitation and emission slit bandwidths of 5 nm. The fluorescence intensities are reported in c.p.s. (counts per second). To check the lamp stability, Raman signals from milli-Q water samples were measured several times during the same day. Comparison of the areas under the Raman scatter peaks (excitation wavelength of 350 nm) revealed no significant changes in the lamp intensity during the measurement period. UV-Vis absorption spectra were recorded on a Helios γ spectrophotometer (Thermo Scientific), using quartz cells of 1.0 cm optical path length. Dissolved organic carbon (DOC) was determined with a Shimadzu model TOC-V CSH apparatus.

Parallel factor analysis (PARAFAC) modelling.

PARAFAC analysis was conducted using MATLAB R2015b (Mathworks, Natick, MA) with the N-way toolbox (http:models.klv.dk/source). A non-negativity constraint was applied to the parameters, thus allowing only chemically relevant results. Some preprocessing steps were adopted to minimize primary and secondary inner-filter effects using the absorption spectra of the samples and the influence of scatter lines.[24] The EEM of a control (Milli-Q water) was subtracted from each sample EEM. Rayleigh and Raman scattering signals were removed according to the protocol described by Bahram et al.[25] PARAFAC models with two to six components were computed for the EEMs. The determination of the correct number of components in the data set was assessed by the core consistency diagnostic score, evaluation of the distribution of residuals and inspection of the physical sense of spectral loadings.

Complexation Modeling

The binding parameters between fluorescent components derived from PARAFAC and Fe(III) were determined using a modification of the complexation model reported by Ryan and Weber[26] using nonlinear fitting of Eq. 1.

$$\frac{I}{I_0} = 1 + \left(\frac{I_{nq}}{I_0} - 1 \right) \frac{\left(KH_0 + KM_0 + 1\right) - \sqrt{\left(KH_0 + KM_0 + 1\right)^2 - 4K^2 H_0 M_0}}{2KH_0} \quad (1)$$

where I_0 is the intensity of SBO solutions without added Fe(III), I is the intensity recorded at a given metal concentration, I_{nq} is the fluorescence intensity that is unaffected by the presence of iron, K denotes the conditional stability constant at a given pH, M_0 is the metal concentration and H_0 is the total concentration of fluorescence-active sites of SBO. Details of Fe(III)-SBO complexation modelling are described in the supplementary information.

Results and discussion

Fluorescence quenching titrations of SBO with Fe(III)

Fluorescence EEMs of SBO recorded at pH 3.0, 5.0 and 7.0 are shown in Figure 1. Similar qualitative EEM contours were observed in all cases, with a well defined peak at excitation/emission (Ex/Em) wavelengths (nm) of 320/430; however, there were quantitative differences, as the fluorescence intensity of EEMs showed a clear dependence on the solution pH and higher values of fluorescence intensity at the 320/430 peak were observed at pH 5. A similar behavior of natural organic matter with pH has also been observed for Yan et al.[27] Although the intrinsic quenching and enhancement mechanism is currently not clear, it has been accepted that carboxylic chromophores significantly contributed to the changes in fluorescence of HS at pH values between 3.0 and 5.0, whereas phenolic chromophores are predominant at pH values between 8.0 and 10.0.[28] In addition, the structure of HS and HLS varies with modifications in their environment as pH changes, which could result in the precipitation of both HS and HLS at pH below 3, thus modifying the recorded fluorescence intensities.[14, 29]

The addition of increasing concentration of Fe(III) to the SBO solution resulted in the decrease of fluorescence intensity for all pH tested, indicating that there is an interaction between both species, which might be interesting to investigate since it could affect the performance of the Fe-HLS photo-Fenton system. For this purpose, the entire set of the EEM data at various Fe(III) concentrations and different pH values was examined using PARAFAC analysis. All the EEMs of the SBO were successfully decomposed into a three-component model. The fluorescence intensities of these components (C1, C2 and C3) at pH 3.0, 5.0 and 7.0 are shown in Figure 2. Each component was tentatively identified with a fraction of organic matter, according to literature data: C1 can be associated with biological degradation of terrestrial humic components[30] and C2 could be linked to humic-like substances from terrestrial

organic matter.[20] In line with the results reported by Ishii and Boyee,[18] the difference between C1 and C2, from a structural viewpoint, may be related to the presence of compounds with larger molecular size and probably more hydrophobic in C2 component. C3 exhibited EEM peaks similar to tryptophan substances derived from sewage DOM.[21] This assignation is meaningful as all three fractions are expected to be found in a system originated from digestion of organic wastes. Finally, the excitation/emission peaks positions were slightly shifted with the increasing pH (Table S1, in supplementary information).

Figure 3 shows the fluorescence quenching curves of each component with the addition of Fe(III) at different pHs. Although marked differences in fluorescent features were observed between fluorophoric components C1 and C2, their fluorescence quenching curves with Fe(III) were similar displaying, in both cases, their highest initial slopes at pH 5. Some quantitative differences could be appreciated, as quenching was more intense for C2. This suggests that certain fluorophores exhibit varying sensitivity to iron aside from properties of aromaticity or molecular weight. The high level of quenching observed for C2 could be the result of either favored iron complexation by humic–like fluorophores of higher molecular weight or greater sensitivity of these fluorophores to fluorescence quenching. Similar findings were reported by Poulin et al.[31] who found that regions of the fluorescence EEM associated with greater DOM conjugation were more susceptible to iron quenching. Opposite trends were observed for the protein-like component (C3); it is well-known that fluorescence of protein-like substances are quenched or enhanced by complexation of metal ions, although the fluorescence quenching method has been scarcely employed to characterize the heavy metal binding potential of specific protein-like substances.[21]

The binding parameters between fluorescent components derived from PARAFAC and Fe(III) were determined using a modification of the complexation model reported by Ryan and Weber as is described in the supplementary information. The stability constants (log K_M) calculated for PARAFAC components, C1 and C2, at pH 3.0, 5.0, 7.0 are listed in Table 1. The log K_M values range from 5.18 to 6.77. These values are slightly higher than those reported in the literature between DOM and Fe(III): log K_M of 4.9-5.3 were determined for DOM from a euthrophic algae-rich lake at pH 6 or log K_M of 5.0 and 5.6 at pH 4.0 for the fulvic acid fraction extracted from composted sewage sludge, municipal wastes, and livestock wastes. [32-33] On the other hand, the stability constant between the Suwannee River Fulvic Acid and Fe(III) at pH 4.0 was reported to be log K = 5.09, also determined by the Ryan and Weber analysis.[34] The stability constant between HLS and Fe(III) should increase with increasing pH from 3 to 7, taking into account that carboxylate groups are involved in formation Fe(III)-HLS complex. However we obtained a maximum value of log K_M for Fe(III)-SBO at pH 5 (Table 1). This could be explained by taking into account differences in speciation of iron, since at increasing pH values the formation of scarcely soluble iron hydroxides is favored; in fact, Mikutta and

Kretzschmar[35] revealed that iron in Fe(III)-HS complexes was predominantly present as oligomeric Fe(III) clusters at neutral pH. Thus, the lower log K_M value at pH 7 with respect to pH 5 could be attributed to the lower affinity of oligomeric Fe(III) species for the carboxylate groups of SBO or to steric hindrance of these bulky molecules. Indeed, the fraction of fluorophores groups that are not quenched by Fe(III) (I_{nq}/I_0) is higher at pH 7 (Table 1). Finally, a lower quenching effect of oligomeric Fe(III) species in comparison with Fe(III) monomeric species could also be expected.

Table 1. Values of log K and f_q for the C1 and C2 with Fe(III) at pH 3, 5 and 7 determined by modified Ryan and Weber model.

pH	C1		C2	
	log K	I_{nq}/I_0	log K	I_{nq}/I_0
3	5.79 ± 0.08	0.43 ± 0.02	6.04 ± 0.09	0.65 ± 0.08
5	6.57 ± 0.06	0.52 ± 0.01	6.77 ± 0.08	0.67 ± 0.02
7	5.18 ± 0.16	0.73 ± 0.07	5.18 ± 0.19	0.82 ± 0.09

Photo-Fenton in the presence of SBO

It is interesting to gain further insight into the behaviour of SBO when submitted to a photo-Fenton process using EEM-PARAFAC. In fact, in a previous work, absorbance spectroscopy combined with organic carbon, chemical oxygen demand and a battery of bioassays, showed that oxidative process resulted in a slight modification of the SBO, which resulted in higher hydrophilicity, and more biocompatible macromolecules.[15] In this work, EEM of solutions of SBO and Fe(III), with and without of H_2O_2, were recorded at different irradiation times and PARAFAC analysis was applied on the respective EEMs data sets. Figure 4 show the change of the three PARAFAC modeled components with irradiation time, at different pH values, in the presence of H_2O_2. Experiments were also carried out in the absence of H_2O_2 (Figure 5) to gain insight regarding the initial photochemical steps involving only Fe(III)-SBO complexes since photo-Fenton processes led to a substantial degradation of SBO. At pH 3 and without of H_2O_2, the fluorescence intensity of all three components decreased with increasing the irradiation time. Formation of a brown precipitate in the solutions at pH 3 was also observed, which could be responsible for the decrease of fluorescence intensity. Furthermore, fluorescence quenching by aggregation of HS in the presence of a cation binding is well-known.[36] TOC measurements showed a substantial decrease in the dissolved organic carbon concentration (about 60% in 10 h) which could account for the precipitate formation at

pH 3. This photo-induced precipitation of SBO-Fe(III) complex at pH 3 may be explained by taking into account the increment of the proportion of carboxyl groups as a result of irradiation, which enhanced the ability of iron to flocculate HLS at pH close to 3. On the other hand, at pH 5 and 7 in the absence of H_2O_2, irradiation resulted in an increase of fluorescence intensity of each component (Figure 4), suggesting a decrease of the fluorescence quenching of SBO by Fe(III). Despite the complexity of the system, a potential explanation for this behavior is that Fe(III)–SBO complexes, under simulated solar-light irradiation, can undergo a charge transfer reactions that result in the formation of Fe(II). This enhanced redox cycling of iron is compatible with the observed ability of SBO to drive photo-Fenton process at pH above 3. In addition, in sharp contrast to the results obtained at pH 3, dissolved organic carbon concentrations measured at pH 5.0 and 7.0 remained constant during the whole irradiation process, most probably because of the higher solubility of HLS at this pH range.

At pH 3, in the presence of H_2O_2, fluorescence intensity of the three derived-components decreased faster than in its absence (compare Figure 4 and 5). Moreover, no evidence of precipitation was found. This may be attributed to the H_2O_2-induced formation of HO radicals that results in a fast SBO degradation within a time scale much shorter than that associated to SBO precipitation. On the contrary, at pH 5 and 7 with H_2O_2, the emission intensity of C1 and C2 increased until reaching maximum values and then decreased to cero at 7 h. DOC measurements, at both pH 5 and 7, only showed a decrease of 20 % after 7 h, indicating that, although SBO fluorophores were degraded, non-fluorescent organic material remained in the solution. This might involve a selective attack of the reactive species towards the fluorophores (e.g. aromatic moieties), generating non-fluorescent more hydrophilic groups, namely carboxylic. The increase in the region of the fluorescence intensity related to C1 and C2 might be connected with the reduction reaction of Fe(III) to Fe(II) from the complex Fe(III)-SBO as stated above. Thus, the maximum position of C1 and C2 that appeared at earlier times at pH 5 than pH 7, may indicate that Fe(III) reduction is a faster processes at pH 5. Since oligomeric Fe(III) species are less photo-reactive than monomeric Fe(III) species,[37] our results are consistent with the hypothesis that, at pH 7, oligomeric Fe(III) cluster are the main Fe(III) species present in the solution with SBO. All these results are in agreement with the loss of efficiency of photo-Fenton above pH 5, suggesting that this is the limit that can be reached following this approach.[12]

Finally, in order to rule out fluorescence changes due to non photo-induced process, dark control experiments were performed. Fluorescence EEMs of samples containing 20 mg L^{-1} of SBO and 5 mg L^{-1} of Fe(III), with and without H_2O_2 (2.2 mmol/L), were recorded during 24 hours in the dark at pH 3.0, 5.0 and 7.0 (data not shown). The analysis of the fluorescence EEMs did not show significant fluorescence changes at the different pH tested, either in the presence or in the absence of H_2O_2. The latter results show that the complexes between Fe(III)

and SBO remain without changes in the absence of irradiation and further suggest that only scarce structural changes occurred because of the inefficiency of dark Fenton process.

Conclusions

The EEM-PARAFAC has been demonstrated as a useful tool for studding mechanistic issues where complex organic molecules, namely HLS, are involved. In particular, complexation of iron(III) with SBO has been studied showing that the strongest Fe(III)-SBO complex is formed at pH = 5, as under more acidic conditions complexation is limited by the protonation of carboxylic groups and at neutral pH values the chemical speciation of Fe(III) hinders its interaction with SBO. Regarding Fe(III)-SBO systems under irradiation at pH 3, it was observed that, in the presence of H_2O_2, the behavior of the system is ruled by the high production of HO radicals rather than the low solubility of the SBO under this conditions. On the other hand, at pH 5 and pH 7, the observed initial increase in the fluorescence can be correlated with the photo-reduction of Fe(III) to Fe(II), thus favoring the photo-Fenton process. Interestingly, the latter increase is faster at pH 5 than at pH 7. Hence, the efficiency decrease observed for photo-Fenton in the presence of SBO above pH 5 can be attributed to the lower complexation of Fe(III) at higher pH, together with the more limited ability to drive iron photo-reduction. Therefore, the results achieved in this paper suggest that the previuosly reported optimal pH for photo-Fenton degradation of EPs in the presence of SBO is closely related to the stability of Fe(III)-SBO complexes formed at different pH values.

Acknowledgements

This work was supported by Generalitat Valenciana, Consellería d'Ecuació, Cultura i esport, Spain (GV/2015/074) and by the Marie Sklodowska-Curie Research and Innovation Staff Exchange project funded by the European Commission H2020-MSCA-RISE-2014 (Project number: 645551). F.S.G.E. and L.C. are researchers from CONICET, Argentina.

Electronic Supplementary Information (ESI) available: Table S1 and details of Fe(III)-HLS complexation modeling.

References

1. S. Malato, P. Fernández-Ibáñez, M. I. Maldonado, J. Blanco and W. Gernjak, Decontamination and disinfection of water by solar photocatalysis: Recent overview and trends, *Catal. Today*, 2009, **147**, 1-59.
2. J. L. Wang and L. J. Xu, Advanced oxidation processes for wastewater treatment: Formation of hydroxyl radical and application, *Crit. Rev. Env. Sci. Tec.*, 2012, **42**, 251-325.

3. J. J. Pignatello, E. Oliveros and A. MacKay, Advanced oxidation processes for organic contaminant destruction based on the Fenton reaction and related chemistry, *Crit. Rev. Env. Sci. Tec.*, 2006, **36**, 1-84.
4. S. Papoutsakis, S. Miralles-Cuevas, I. Oller, J. L. Garcia Sanchez, C. Pulgarin and S. Malato, Microcontaminant degradation in municipal wastewater treatment plant secondary effluent by EDDS assisted photo-Fenton at near-neutral pH: An experimental design approach, *Catal. Today*, 2015, **252**, 61-69.
5. N. Klamerth, S. Malato, A. Agüera and A. Fernández-Alba, Photo-Fenton and modified photo-Fenton at neutral pH for the treatment of emerging contaminants in wastewater treatment plant effluents: A comparison, *Water Res.*, 2013, **47**, 833-840.
6. A. De Luca, R. F. Dantas and S. Esplugas, Study of Fe(III)-NTA chelates stability for applicability in photo-Fenton at neutral pH, *Appl. Cat. B: Environ.*, 2015, **179**, 372-379.
7. A. Bernabeu, S. Palacios, R. Vicente, R. F. Vercher, S. Malato, A. Arques and A. M. Amat, Solar photo-Fenton at mild conditions to treat a mixture of six emerging pollutants, *Chem. Eng. J.*, 2012, **198-199**, 65-72.
8. N. Klamerth, S. Malato, M. I. Maldonado, A. Agüera and A. Fernández-Alba, Modified photo-Fenton for degradation of emerging contaminants in municipal wastewater effluents, *Catal. Today*, 2011, **161**, 241-246.
9. B. M. Voelker, F. M. M. Morel and B. Sulzberger, Iron Redox Cycling in Surface Waters: Effects of Humic Substances and Light, *Environ. Sci. Technol.*, 1997, **31**, 1004-1011.
10. N. De la Cruz, J. Giménez, S. Esplugas, D. Grandjean, L. F. de Alencastro and C. Pulgarín, Degradation of 32 emergent contaminants by UV and neutral photo-fenton in domestic wastewater effluent previously treated by activated sludge, *Water Res.*, 2012, **46**, 1947-1957.
11. J. Gomis, R. F. Vercher, A. M. Amat, D. O. Mártire, M. C. González, A. Bianco Prevot, E. Montoneri, A. Arques and L. Carlos, Application of soluble bio-organic substances (SBO) as photocatalysts for wastewater treatment: Sensitizing effect and photo-Fenton-like process, *Catal. Today*, 2013, **209**, 176-180.
12. J. Gomis, L. Carlos, A. B. Prevot, A. C. S. C. Teixeira, M. Mora, A. M. Amat, R. Vicente and A. Arques, Bio-based substances from urban waste as auxiliaries for solar photo-Fenton treatment under mild conditions: Optimization of operational variables, *Catal. Today*, 2015, **240, Part A**, 39-45.
13. J. Gomis, A. Bianco Prevot, E. Montoneri, M. C. González, A. M. Amat, D. O. Mártire, A. Arques and L. Carlos, Waste sourced bio-based substances for solar-driven wastewater remediation: Photodegradation of emerging pollutants, *Chem. Eng. J.*, 2014, **235**, 236-243.
14. P. Avetta, S. Berto, A. Bianco Prevot, M. Minella, E. Montoneri, D. Persico, D. Vione, M. C. Gonzalez, D. O. Mártire, L. Carlos and A. Arques, Photoinduced transformation of waste-derived soluble bio-based substances, *Chem. Eng. J.*, 2015, **274**, 247-255.
15. J. Gomis, M. G. Gonçalves, R. F. Vercher, C. Sabater, M.-A. Castillo, A. B. Prevot, A. M. Amat and A. Arques, Determination of photostability, biocompatibility and efficiency as photo-Fenton auxiliaries of three different types of soluble bio-based substances (SBO), *Catal. Today*, 2015, **252**, 177-183.
16. A. M. Berkovic, F. S. García Einschlag, M. C. Gonzalez, R. Pis Diez and D. O. Mártire, Evaluation of the Hg2+ binding potential of fulvic acids from fluorescence excitation-emission matrices, *Photochem. Photobiol. Sci.*, 2013, **12**, 384-392.
17. C. A. Stedmon and R. Bro, Characterizing dissolved organic matter fluorescence with parallel factor analysis: A tutorial, *Limnology and Oceanography: Methods*, 2008, **6**, 572-579.

18. S. K. L. Ishii and T. H. Boyer, Behavior of Reoccurring PARAFAC Components in Fluorescent Dissolved Organic Matter in Natural and Engineered Systems: A Critical Review, *Environ. Sci. Technol.*, 2012, **46**, 2006-2017.
19. Y. Su, F. Chen and Z. Liu, Comparison of optical properties of chromophoric dissolved organic matter (CDOM) in alpine lakes above or below the tree line: insights into sources of CDOM, *Photochem. Photobiol. Sci.*, 2015, **14**, 1047-1062.
20. X. Yang, F. Meng, G. Huang, L. Sun and Z. Lin, Sunlight-induced changes in chromophores and fluorophores of wastewater-derived organic matter in receiving waters - The role of salinity, *Water Res.*, 2014, **62**, 281-292.
21. J. Wu, H. Zhang, P. J. He and L. M. Shao, Insight into the heavy metal binding potential of dissolved organic matter in MSW leachate using EEM quenching combined with PARAFAC analysis, *Water Res.*, 2011, **45**, 1711-1719.
22. Y. Yamashita and R. Jaffé, Characterizing the interactions between trace metals and dissolved organic matter using excitation-emission matrix and parallel factor analysis, *Environ. Sci. Technol.*, 2008, **42**, 7374-7379.
23. R. Nisticò, M. Barrasso, G. A. CarrilloLeRoux, M. M. Seckler, W. Sousa, M. Malandrino and G. Magnacca, Biopolymers from Composted Biowaste as Stabilizers for the Synthesis of Spherical and Homogeneously Sized Silver Nanoparticles for Textile Applications on Natural Fibers, *ChemPhysChem*, 2015, **16**, 3902-3909.
24. T. Ohno, Fluorescence inner-filtering correction for determining the humification index of dissolved organic matter, *Environ. Sci. Technol.*, 2002, **36**, 742-746.
25. M. Bahram, R. Bro, C. Stedmon and A. Afkhami, Handling of Rayleigh and Raman scatter for PARAFAC modeling of fluorescence data using interpolation, *Journal of Chemometrics*, 2006, **20**, 99-105.
26. D. K. Ryan and J. H. Weber, Fluorescence quenching titration for determination of complexing capacities and stability constants of fulvic acid, *Anal. Chem.*, 1982, **54**, 986-990.
27. M. Yan, Q. Fu, D. Li, G. Gao and D. Wang, Study of the pH influence on the optical properties of dissolved organic matter using fluorescence excitation–emission matrix and parallel factor analysis, *Journal of Luminescence*, 2013, **142**, 103-109.
28. D. J. Dryer, G. V. Korshin and M. Fabbricino, In Situ Examination of the Protonation Behavior of Fulvic Acids Using Differential Absorbance Spectroscopy, *Environ. Sci. Technol.*, 2008, **42**, 6644-6649.
29. K. Ghosh and M. Schnitzer, Fluorescence Excitation Spectra and Viscosity Behavior of a Fulvic Acid and its Copper and Iron Complexes1, *Soil Science Society of America Journal*, 1981, **45**, 25-29.
30. B. A. Lyon, R. M. Cory and H. S. Weinberg, Changes in dissolved organic matter fluorescence and disinfection byproduct formation from UV and subsequent chlorination/chloramination, *J. Hazard. Mater.*, 2014, **264**, 411-419.
31. B. A. Poulin, J. N. Ryan and G. R. Aiken, Effects of Iron on Optical Properties of Dissolved Organic Matter, *Environ. Sci. Technol.*, 2014, **48**, 10098-10106.
32. H. Xu, Z. Yan, H. Cai, G. Yu, L. Yang and H. Jiang, Heterogeneity in metal binding by individual fluorescent components in a eutrophic algae-rich lake, *Ecotox. Environ. Safety*, 2013, **98**, 266-272.
33. J. C. G. Esteves Da Silva, A. A. S. C. MacHado, C. J. S. Oliveira and M. S. S. D. S. Pinto, Fluorescence quenching of anthropogenic fulvic acids by Cu(II), Fe(III) and UO2/2+, *Talanta*, 1998, **45**, 1155-1165.
34. J. Zhao and D. J. Nelson, Fluorescence study of the interaction of Suwannee River fulvic acid with metal ions and Al 3+-metal ion competition, *Journal of Inorganic Biochemistry*, 2005, **99**, 383-396.
35. C. Mikutta and R. Kretzschmar, Spectroscopic evidence for ternary complex formation between arsenate and ferric iron complexes of humic substances, *Environ. Sci. Technol.*, 2011, **45**, 9550-9557.

36. S. Orsetti, J. L. Marco-Brown, E. M. Andrade and F. V. Molina, Pb(II) Binding to Humic Substances: An Equilibrium and Spectroscopic Study, *Environ. Sci. Technol.*, 2013, **47**, 8325-8333.

37. L. Lopes, J. de Laat and B. Legube, Charge Transfer of Iron(III) Monomeric and Oligomeric Aqua Hydroxo Complexes: Semiempirical Investigation into Photoactivity, *Inorg. Chem.*, 2002, **41**, 2505-2517.

Figures

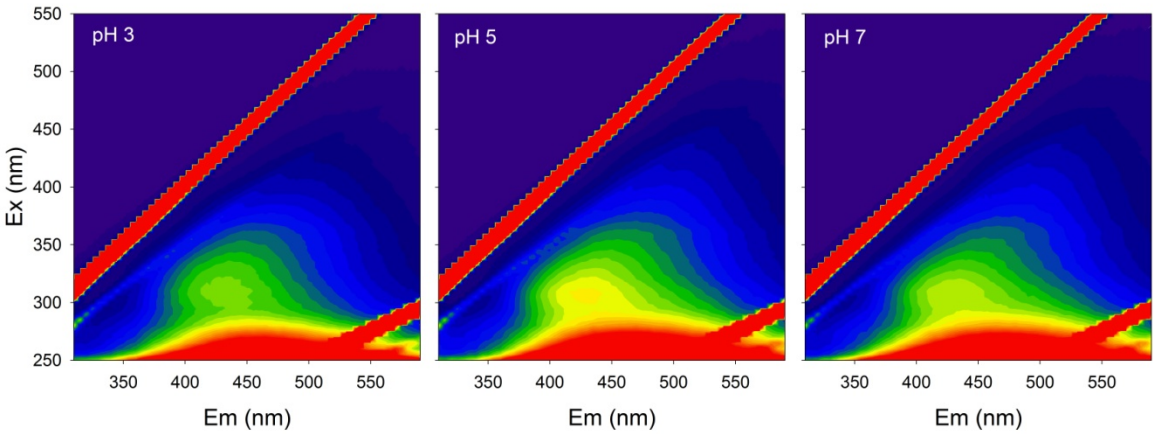

Figure 1. Fluorescence EEMs of SBO (20 mg L^{-1}) at different pH.

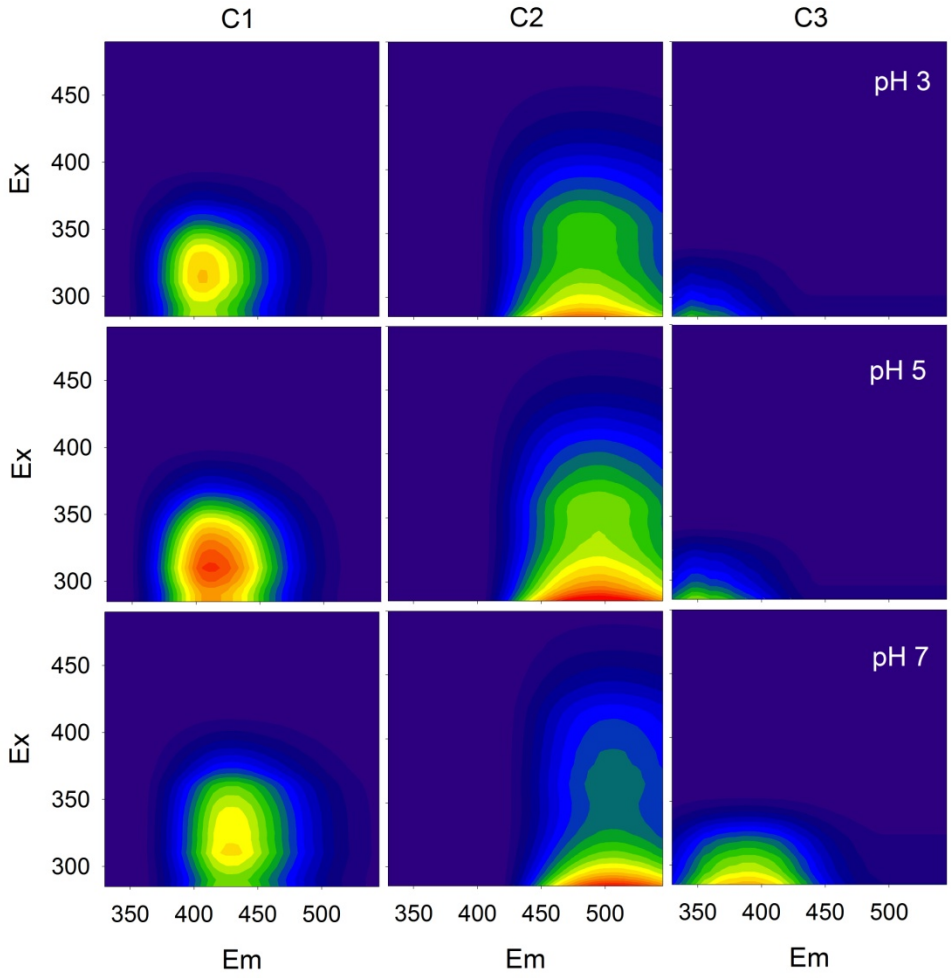

Figure 2. Fluorescence EEMs of the three components identified by PARAFAC model at pH different pH.

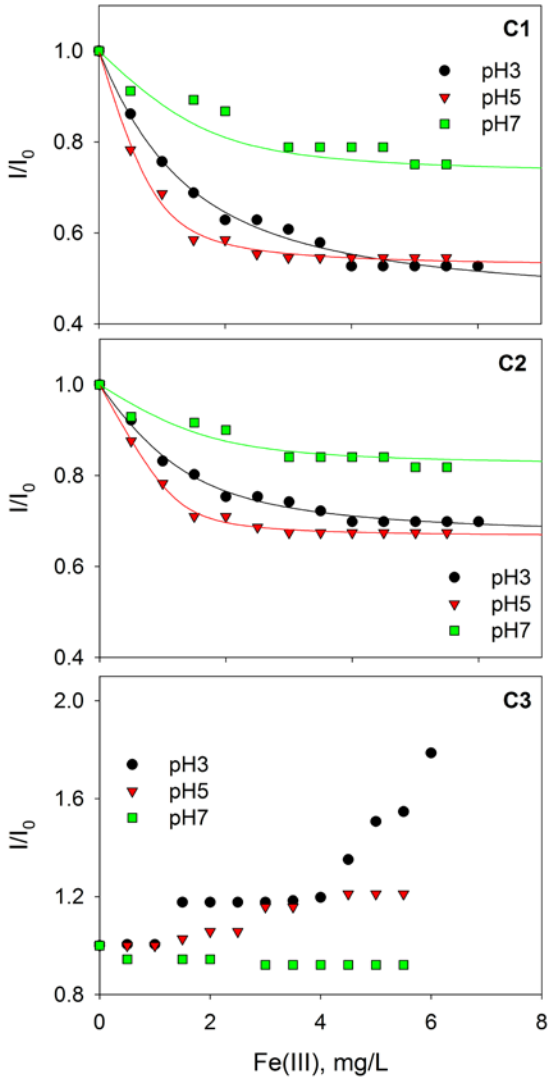

Figure 3. Changes in the relative fluorescence intensity of three PARAFAC-derived components with the addition of Fe(III) at pH 3.0, 5.0 and 7.0. Lines represent fittings to the Ryan–Weber equation.

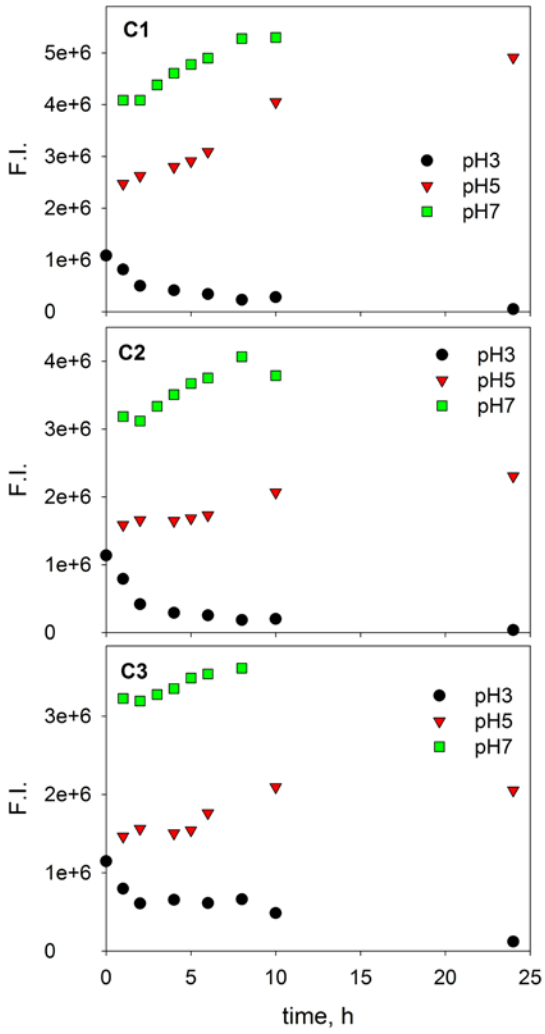

Figure 4. Changes in the fluorescence intensity of three PARAFAC-derived components with the irradiation time for SBO with Fe(III) at pH 3.0, 5.0 and 7.0. $[SBO]_0$ = 20 mg L^{-1}; $[Fe(III)]_0$ = 20 mg L^{-1}.

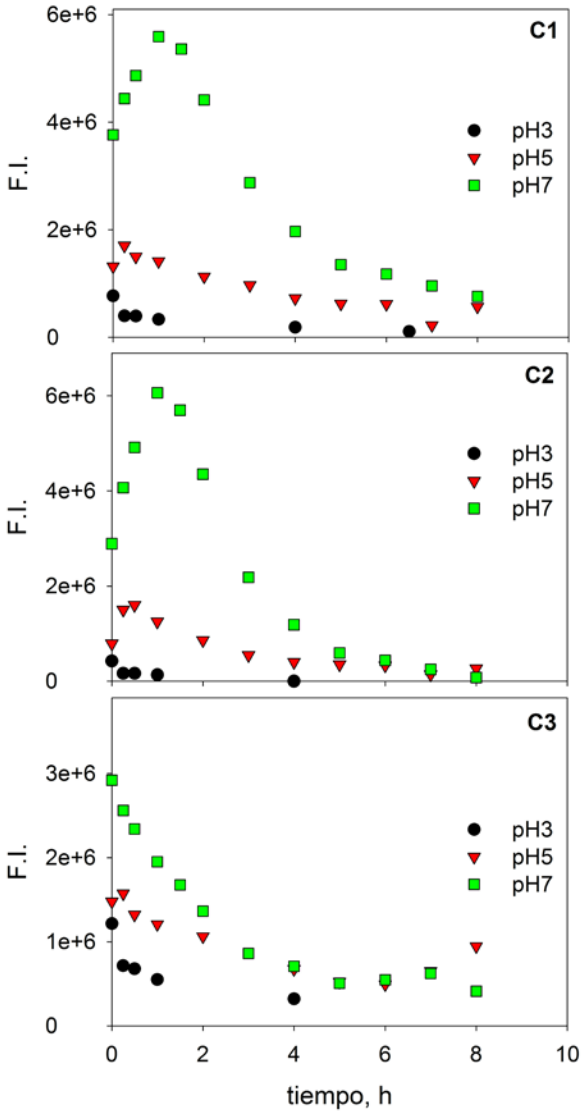

Figure 5. Changes in the fluorescence intensity of three PARAFAC-derived components with the irradiation time for SBO with Fe(III) and H_2O_2 at pH 3.0, 5.0 and 7.0. $[SBO]_0$ = 20 mg L^{-1}; $[Fe(III)]_0$ = 20 mg L^{-1}; $[H_2O_2]_0$ = 2.2 mmol L^{-1}.